Aportaciones Matemáticas
Comunicaciones **23** (1999) 13–48.

Vacuum moulding of a superplastic

S. J. Chapman* A. D. Fitt† G. Pulos

October 14, 1997

1 Introduction

Superplasticity in metals and alloys is a phenomenon that has attracted the attention of people from the scientific as well as the industrial communities for the past 30 years. More recently, superplastic behavior has been studied in intermetallics, ceramics and metal matrix composites.

Superplastic behavior is characterized by very large (plastic) deformations on the order of 200 to over a few thousand percent (regular plastic deformations range from less than 1% to about 80%). From a Materials Science point of view the requirement for superplasticity is a small grain size (less than 10 microns); in this case, for temperatures around 1/2 of the melting temperature and for deformation rates that go between 10^{-3}/s for grains around 10 microns to 10/s for grains about 0.5 microns [7], materials are able to undergo large deformations without failure. Apparently, the small grain size allows grain boundary sliding to occur while cavitation is delayed. Void formation and coalescence as a precursor to microcracking is a typical failure mechanism in ductile materials.

From an industrial point of view, superplasticity brings several advantages to material forming technology. The manufacturing of complex shaped pieces can be accomplished with low pressures, without any welding and with minimal or no subsequent machining. As with any thin wall structure, the strength and failure load (considering bucking, for example) will depend critically on the local curvature and thickness.

The motivation for this work comes from the experimental work of Professor Torres (Instituto de Investigaciones en Materiales, UNAM) on two superplastic systems. The materials used in the experiments were a Cadmium-Zinc alloy and Zinalco, a 77% Zinc, 21% Aluminum & 2% Copper alloy developed by Professor Torres and his group Experiments were carried out on the behavior of hemispheric free-bulging from sheets as well as vacuum moulding in a circular cylindrical mould with a depth between 1 and 1.3 diameters (representing deformations around 200 to 250%). The hemispherical bulging can be considered

*Mathematical Institute, 24-29 St. Giles, Oxford OX1 3LB, UK. Supported by A Royal Society Research Fellowship

†Faculty of Mathematical Studies, University of Southampton

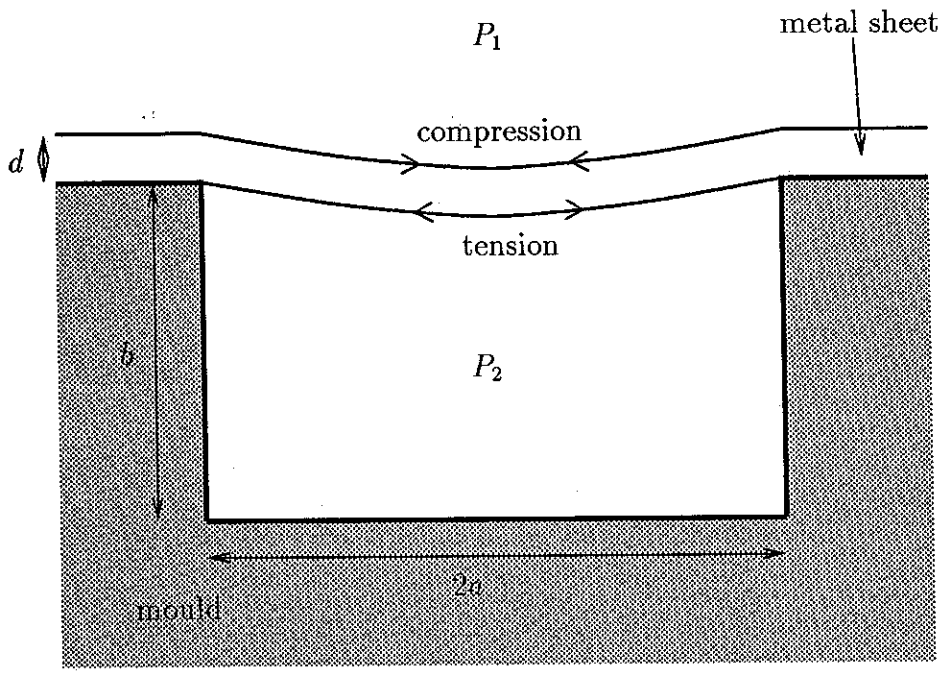

Figure 1: The geometry of the sheet

the first part of the vacuum moulding experiment where the superplastic has not reached the walls of the mould

The objective of this research is to develop a model for simulating the superplastic forming process and for predicting the thickness distribution as well the minimum radius of curvature when the material has to fill a sharp corner. Other questions of interest are the deflection of the sheet as a function of pressure for a given mould opening, and the deflection as a function of mould diameter for a given pressure Modeling based on shell theory is carried out for cylindrical, spherical and arbitrary-shape shells of uniform as well as non-uniform thicknesses.

Before detailing the methodology used, it is worth considering how one can use shell theory (small deformations theory) to simulate the vacuum forming process.

Starting with a flat sheet of metal clamped to a circular mould of diameter $2a$ and depth b ($b > a$, initial uniform thickness $d \sim 0.02a$) under differential pressure, the problem corresponds to that of a flat plate where the out of plane loading (uniform pressure) is resisted by bending stresses (in-plane stresses); the concave surface is under compression while the convex surface is under tension (see Figure 1) Thus, the initial configuration problem can be described by plate theory (2 Dimensional beam theory); however, ordinary plate theory can only

To extend the analysis, it is necessary to use von Karman plate theory (a non-linear theory) which includes the effect of in-plane stresses and can be used for larger deflections; in this case, the out of plane loads are carried by in-plane bending stresses in combination with membrane (i.e. tensile) hoop stresses.

The transition from plate theory to shell theory in which a curved geometry can carry out-of-plane loads by hoop stresses (positive throughout the thickness) comes after a plastic hinge forms on the rim of the mould.

The effect of a plastic hinge can be understood by considering a cantilever beam under uniform pressure. There is a pressure that induces the formation of plastic zones at the built-in end; the plastic zones form on the top and bottom surfaces are separated by an elastic core. As the pressure is increased the plastic zones grow inwardly until they meet when the thickness of the elastic core is reduced to zero. This configuration is called a plastic hinge and it allows unrestrained plastic deformation that turns the clamped boundary condition into a moment-free boundary condition [5]. For the clamped plate, the plastic hinge also marks the transition from plate to shell theory as the unrestrained plastic flow allows the redistribution of stresses to a purely tensile hoop stress distribution; in this case, the out of plane pressure loading is resisted by membrane stresses. Of course, one would have to examine this situation numerically to make definitive statements about the transition of the stress distributions.

Assuming this is the case, the new configuration is that of a curved (elastic) geometry of uniform thickness and under uniform pressure; the boundary conditions are zero displacement and moment and are applied at the circular rim. Under these considerations one would expect that the problem is adequately described by a spherical shell. This has been confirmed by experimental observations.

In this context, the analysis of an elasto-plastic shell becomes relevant. There, as the pressure is increased the initial yield pressure is reached, at which the material adjacent to the concave surface becomes plastic. However, it is held in place by the outer elastic sheath, and so cannot flow (see Figure 2). Flow will only take place when the material becomes fully plastic, which will happen for some higher value of the pressure. For a spherical shell, once it is fully plastic there is no stable equilibrium configuration for an infinitesimal increment of pressure since as the shell expands it has a larger radius of curvature, which (as we will see) gives it a lower ability to resist the internal pressure. However, for a constrained shell (in this case by the rim of the mould), if the shell re-shapes into a geometry with a smaller radius of curvature then there is a stable equilibrium configuration even for a shell with reduced thickness (as an isochoric plastic deformation rule would dictate). It is this concept of a sequence of quasi-static change of equilibrium configuration which motivates the use of small deformation shell theory to model the process even though the deformations may be on the order of 250%.

In the following, elastic-plastic shell analysis is applied to circularly cylindrical and spherical shells in sections 2 and 3 while section 4 considers uniform

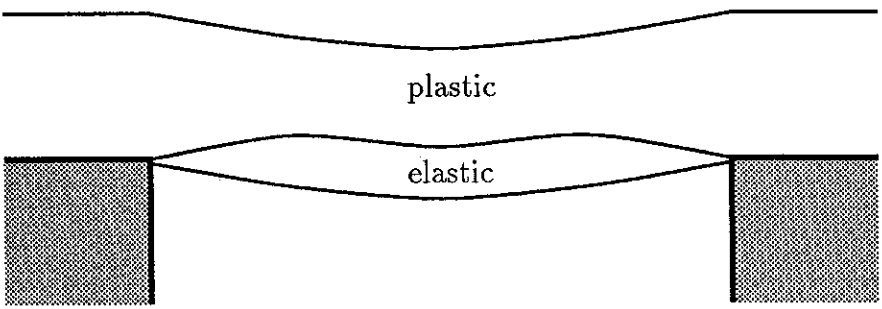

Figure 2: Schematic diagram showing the elastic and plastic regions of the sheet between the yield pressure (at which the plastic region first forms) and the flow pressure (at which the sheet is fully plastic).

the quasi-static change of equilibrium configurations is used to model the evolution of the sheet in 2 dimensions in section 6 while the 3 dimensional case is considered in section 7; the non-uniform thinning case is considered in section 8.

It is clear that in all of the plasticity modeling time enters as a parameter that is useful for incremental calculations but cannot be related to real-time unless a viscous constitutive law is used. Section 9 considers the modeling of the superplastic as a viscous fluid. While this point of view offers the advantages that time-dependent processes as well as large deformations (small flow rates) can now be modeled, it is shown that the equations are much harder to solve. Finally, some conclusions are drawn in section 10.

This section finishes with the equations governing plastic yield. We will assume that the material is a perfect plastic, so that its stress/strain relationship is as shown in Figure 3.

Let the stress tensor be denoted by σ_{ij}. This may be written as a sum of the *hydrostatic* stress $\sigma_{kk}\delta_{ij}/3$ (we use the summation convention throughout) and the *deviatoric* stress

$$\sigma'_{ij} = \sigma_{ij} - \sigma_{kk}\delta_{ij}/3.$$

Note that $\sigma'_{kk} = 0$. The Von-Mises yield condition for a perfect plastic material may be written as [4]

$$\sigma'_{ij}\sigma'_{ij} = \frac{2\sigma_Y^2}{3}, \tag{1}$$

where σ_Y is the yield stress of the material in pure tension.

Coordinate axes may always be chosen so that the stress tensor is diagonal; the coordinate directions are then known as the principal directions and the diagonal entries in the stress tensor as the principal stresses. Let the stress tensor in the principal coordinate system be denoted by τ_{ij}. Then the Von-Mises

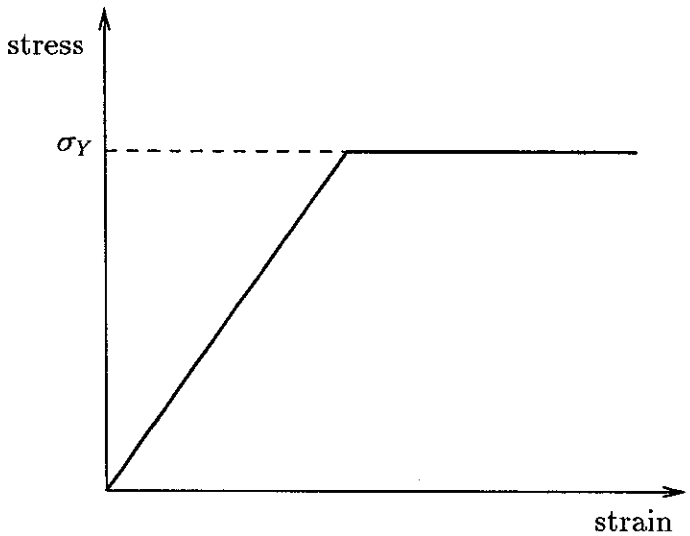

Figure 3: Stress-strain curve for an elastic/perfect plastic material.

condition (1) may be written in terms of the deviatoric part of the principal stress tensor as (see, for example [2, 4])

$$(\tau'_{11})^2 + (\tau'_{22})^2 + (\tau'_{33})^2 = \frac{2\sigma_Y^2}{3}. \tag{2}$$

This may be rewritten in many ways. Perhaps the most convenient is

$$(\tau_{11} - \tau_{22})^2 + (\tau_{11} - \tau_{33})^2 + (\tau_{22} - \tau_{33})^2 = 2\sigma_Y^2. \tag{3}$$

An alternative plastic yield condition is that due to Tresca, which is

$$\max(|\tau_{11} - \tau_{22}|, |\tau_{11} - \tau_{33}|, |\tau_{22} - \tau_{33}|) = \sigma_Y \tag{4}$$

In three dimensions these two conditions turn out to be equivalent for the situations we consider.

In two dimensions $\tau'_{33} = 0$, which implies $\tau_{33} = (\tau_{11} + \tau_{22})/2$. Then the Von-Mises condition becomes

$$(\tau_{11} - \tau_{22})^2 = \frac{4\sigma_Y^2}{3}, \tag{5}$$

while the Tresca condition becomes

$$|\tau_{11} - \tau_{22}| = \sigma_Y. \tag{6}$$

2 Circularly cylindrical shell

In this section we consider the problem of "blowing up" an elastic/plastic cylindrical shell by imposing a slowly increasing internal pressure. We assume that the displacement of the material is radial. Then the equations for the stress become

$$\sigma_{r\theta} = 0, \tag{7}$$

$$r\frac{\partial \sigma_{rr}}{\partial r} + \sigma_{rr} - \sigma_{\theta\theta} = 0, \tag{8}$$

with σ_{rr} and $\sigma_{\theta\theta}$ fuunctions of r only. While the material is elastic, the stresses are given in terms of the radial displacement u_r by

$$\sigma_{rr} = (\lambda + 2\mu)\frac{\partial u_r}{\partial r} + \lambda\frac{u_r}{r}, \tag{9}$$

$$\sigma_{\theta\theta} = \lambda\frac{\partial u_r}{\partial r} + (\lambda + 2\mu)\frac{u_r}{r} \tag{10}$$

The boundary conditions on these equations are

$$\sigma_{rr}(a) = -P, \tag{11}$$

$$\sigma_{rr}(b) = 0, \tag{12}$$

where a and b are the inner and outer radii of the cylinder respectively. With the Tresca yield condition, we also have the constraint that $|\sigma_{rr} - \sigma_{\theta\theta}| < \sigma_Y$ for the material to remain elastic (the results for a Von-Mises yield condition may be obtained by simply replacing σ_Y with $2\sigma_Y/\sqrt{3}$). Substituting (9), (10) into (8) gives

$$r\frac{\partial^2 u_r}{\partial r^2} + \frac{\partial u_r}{\partial r} - \frac{u_r}{r} = 0. \tag{13}$$

Hence

$$u_r = Ar + \frac{B}{r}, \tag{14}$$

giving

$$\sigma_{rr} = 2(\lambda + \mu)A - \frac{2\mu B}{r^2}, \tag{15}$$

$$\sigma_{\theta\theta} = 2(\lambda + \mu)A + \frac{2\mu B}{r^2}. \tag{16}$$

Applying the boundary conditions gives

$$A = \frac{a^2 P}{2(\lambda + \mu)(b^2 - a^2)}, \tag{17}$$

$$B = \frac{a^2 b^2 P}{2\mu(b^2 - a^2)}. \tag{18}$$

Hence

$$\sigma_{rr} = -\frac{a^2P}{(b^2-a^2)}\left(\frac{b^2}{r^2}-1\right), \tag{19}$$

$$\sigma_{\theta\theta} = \frac{a^2P}{(b^2-a^2)}\left(\frac{b^2}{r^2}+1\right). \tag{20}$$

Then $\Delta = \sigma_{\theta\theta} - \sigma_{rr}$ is given by

$$\Delta = \frac{2a^2b^2P}{r^2(b^2-a^2)}. \tag{21}$$

This is largest on the inner radius, where it is equal to

$$\Delta_a = \frac{2b^2P}{(b^2-a^2)}. \tag{22}$$

Thus the cylinder will start to become plastic when the pressure inside reaches the value P_Y given by

$$P_Y = \frac{\sigma_Y(b^2-a^2)}{2b^2}. \tag{23}$$

For pressures above this value the material comprises a plastic annulus inside an elastic sheath. Let the plastic annulus be $a < r < c$ and the elastic sheath be $c < r < b$. Then equations (9), (10) and (13) still hold for $c < r < b$, while in $a < r < c$ we have equations (7) and (8) with the additional condition that

$$\sigma_{\theta\theta} - \sigma_{rr} = \sigma_Y. \tag{24}$$

Hence, for $a < r < c$ we can integrate (8) immediately to give

$$\sigma_{rr} = \sigma_Y \log r + C, \qquad a < r < c. \tag{25}$$

Applying the boundary condition on $r = a$ gives

$$C = -P - \sigma_Y \log a, \tag{26}$$

and hence

$$\sigma_{rr} = -P + \sigma_Y(\log r - \log a), \qquad a < r < c, \tag{27}$$

$$\sigma_{\theta\theta} = -P + \sigma_Y(\log r - \log a + 1), \qquad a < r < c. \tag{28}$$

In the elastic region we still have the solution (14)-(16) (with different values of A and B). The stresses must be continuous across $r = c$, and we still have zero normal stress at $r = b$ These conditions give the equations

$$2(\lambda+\mu)A - \frac{2\mu B}{b^2} = 0, \tag{29}$$

$$2(\lambda+\mu)A - \frac{2\mu B}{c^2} = -P + \sigma_Y(\log c - \log a), \tag{30}$$

$$2(\lambda+\mu)A - \frac{2\mu B}{\quad} \tag{31}$$

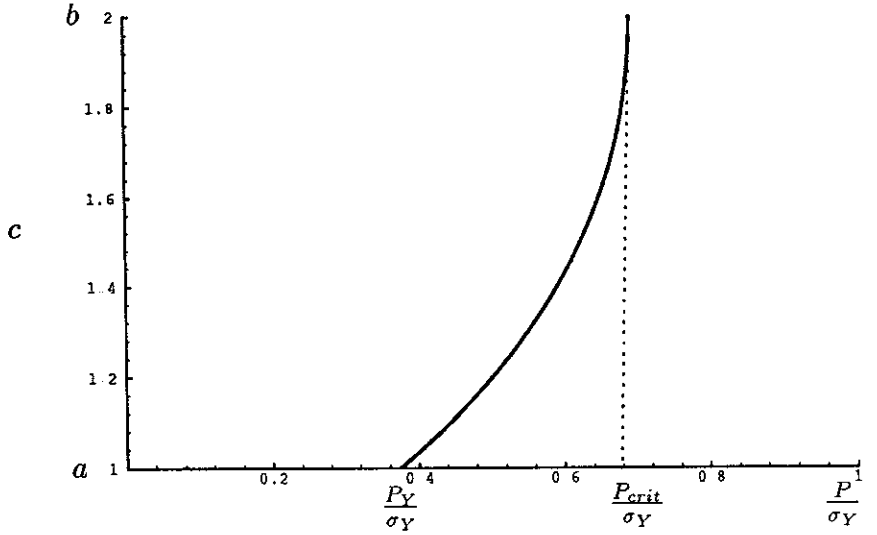

Figure 4: The boundary of the plastic region, c, as a function of the pressure P.

for A, B and the free boundary position c. Eliminating A and B gives the following transcendental equation for c

$$\frac{P}{\sigma_Y} = \log(c/a) + \frac{b^2 - c^2}{2b^2}, \tag{32}$$

which is shown in Figure 4 for $a = 1$, $b = 2$. The right-hand side of this equation is increasing for c between a and b. Thus, as P increases above P_Y the free boundary moves from $c = a$ to eventually reach $c = b$ at the value

$$P = P_{crit} = \sigma_Y \log(b/a). \tag{33}$$

For values of P above P_{crit} the cylinder will flow plastically and will burst

To motivate the asymptotics to follow, let us examine this exact elastic solution in the limit $b - a \ll 1$. Let $b = a + \epsilon d$, $r = a + \epsilon\rho$, $\epsilon \ll 1$. Then, from (19), (20) we see that

$$\sigma_{rr} \sim -\frac{P(d-\rho)}{d}, \tag{34}$$

$$\sigma_{\theta\theta} \sim \frac{aP}{\epsilon d}, \tag{35}$$

while from (23) we see that P_Y is given by

$$P_Y = \frac{\sigma_Y \epsilon d}{a} \tag{36}$$

Thus we see that the pressure required to generate a plastic zone is $O(\epsilon)$, and

Let us now examine the plastic/elastic solution. From (33) we see that to leading order

$$P_{crit} \sim \frac{\sigma_Y \epsilon d}{a} \tag{37}$$

Thus $P_{crit} = P_Y$ to leading order in ϵ and we must go to second order to examine the transition from purely elastic to purely plastic. Therefore we set $P = \epsilon\sigma_Y d/a + \epsilon^2 \bar{P}$. We also let $c = a + \epsilon\bar{c}$. Then, to leading order throughout the sheet the solution (34), (35) holds. The quantity of interest is $\bar{c}$, which identifies the point of plastic/elastic transition. Expanding (23) and (33) to two terms gives

$$P_Y \sim \frac{\sigma_Y \epsilon d}{a} - \frac{3\sigma_Y \epsilon^2 d^2}{2a^2}, \tag{38}$$

$$P_{crit} \sim \frac{\sigma_Y \epsilon d}{a} - \frac{\sigma_Y \epsilon^2 d^2}{2a^2} \tag{39}$$

From (32) we find that $\bar{c}$ is given in terms of $\bar{P}$ by

$$\frac{\bar{P}}{\sigma_Y} \sim -\frac{(\bar{c}-d)^2}{a^2} - \frac{d^2}{2a^2} \tag{40}$$

3 Spherical shell

Here we consider the problem of blowing up a spherical shell of elastic/plastic material by imposing a slowly increasing internal pressure. We assume that the displacement is in the radial direction and a function of r only. Then the equations for the stress become

$$\sigma_{r\phi} = \sigma_{r\theta} = \sigma_{\phi\theta} = 0, \tag{41}$$

$$\sigma_{\theta\theta} = \sigma_{\phi\phi}, \tag{42}$$

$$\frac{d}{dr}(r^2\sigma_{rr}) - r\sigma_{\theta\theta} - r\sigma_{\phi\phi} = 0 \tag{43}$$

In the elastic regime the stresses are given in terms of the radial displacement u_r by

$$\sigma_{rr} = (\lambda + 2\mu)\frac{du_r}{dr} + 2\lambda\frac{u_r}{r}, \tag{44}$$

$$\sigma_{\theta\theta} = \lambda\frac{du_r}{dr} + 2(\lambda+\mu)\frac{u_r}{r}, \tag{45}$$

$$\sigma_{\phi\phi} = \lambda\frac{du_r}{dr} + 2(\lambda+\mu)\frac{u_r}{r} \tag{46}$$

The boundary conditions, as before, are

$$(47)$$

where a and b are the inner and outer radii of the cylinder respectively. Using (42) we find the Tresca constraint for the material to remain elastic,

$$|\sigma_{rr} - \sigma_{\theta\theta}| < \sigma_Y, \tag{49}$$

is equivalent to the Von-Mises constraint

$$(\sigma_{rr} - \sigma_{\theta\theta})^2 + (\sigma_{rr} - \sigma_{\phi\phi})^2 + (\sigma_{\phi\phi} - \sigma_{\theta\theta})^2 < 2\sigma_Y^2. \tag{50}$$

Substituting (44)-(46) into (43) gives

$$r^2 \frac{\partial^2 u_r}{\partial r^2} + 2r \frac{\partial u_r}{\partial r} - 2u_r = 0 \tag{51}$$

Hence

$$u_r = Ar + \frac{B}{r^2}, \tag{52}$$

giving

$$\sigma_{rr} = (3\lambda + 2\mu)A - \frac{4\mu B}{r^3}, \tag{53}$$

$$\sigma_{\theta\theta} = (3\lambda + 2\mu)A + \frac{2\mu B}{r^3}, \tag{54}$$

$$\sigma_{\phi\phi} = (3\lambda + 2\mu)A + \frac{2\mu B}{r^3}. \tag{55}$$

Applying the boundary conditions gives

$$A = \frac{a^3 P}{(3\lambda + 2\mu)(b^3 - a^3)}, \tag{56}$$

$$B = \frac{a^3 b^3 P}{4\mu(b^3 - a^3)}. \tag{57}$$

Hence

$$\sigma_{rr} = -\frac{a^3 P}{(b^3 - a^3)} \left(\frac{b^3}{r^3} - 1 \right), \tag{58}$$

$$\sigma_{\theta\theta} = \frac{a^3 P}{(b^3 - a^3)} \left(\frac{b^3}{2r^3} + 1 \right), \tag{59}$$

$$\sigma_{\phi\phi} = \frac{a^3 P}{(b^3 - a^3)} \left(\frac{b^3}{2r^3} + 1 \right). \tag{60}$$

Then $\Delta = \sigma_{\theta\theta} - \sigma_{rr}$ is given by

$$\Delta = \frac{a^3 P}{(b^3 - a^3)} \frac{2\sqrt{2} b^3}{r^3} \tag{61}$$

This is largest on the inner radius, where it is equal to

Thus the cylinder will start to become plastic when the pressure inside reaches the value P_Y given by

$$P_Y = \frac{2(b^3 - a^3)\sigma_Y}{3b^3}. \tag{63}$$

For pressures above this value the material again comprises a plastic shell inside an elastic sheath. Let the plastic shell be $a < r < c$ and the elastic sheath be $c < r < b$. Then equations (44)-(46) and (51) still hold for $c < r < b$, while in $a < r < c$ we have equations (42) and (43) with the additional condition that

$$\Delta = \sigma_Y. \tag{64}$$

Hence, for $a < r < c$ we can also integrate (43) immediately to give

$$\sigma_{rr} = 2\sigma_Y \log r + C, \qquad a < r < c. \tag{65}$$

Applying the boundary condition on $r = a$ gives

$$C = -P - 2\sigma_Y \log a, \tag{66}$$

and hence

$$\sigma_{rr} = -P + 2\sigma_Y(\log r - \log a), \qquad a < r < c, \tag{67}$$

$$\sigma_{\theta\theta} = -P + 2\sigma_Y(\log r - \log a + 1/2), \qquad a < r < c, \tag{68}$$

$$\sigma_{\phi\phi} = -P + 2\sigma_Y(\log r - \log a + 1/2), \qquad a < r < c. \tag{69}$$

In the elastic region we still have the solution (53)-(55) (with different values of A and B). The stresses must be continuous across $r = c$, and we still have zero normal stress at $r = b$. These conditions give the equations

$$(3\lambda + 2\mu)A - \frac{4\mu B}{b^3} = 0, \tag{70}$$

$$(3\lambda + 2\mu)A - \frac{4\mu B}{c^3} = -P + 2\sigma_Y(\log c - \log a), \tag{71}$$

$$(3\lambda + 2\mu)A + \frac{2\mu B}{c^3} = -P + 2\sigma_Y(\log c - \log a + 1/2), \tag{72}$$

for A, B and the free boundary position c. Eliminating A and B gives the following transcendental equation for c:

$$\frac{P}{\sigma_Y} = 2\log(c/a) + \frac{2(b^3 - c^3)}{3b^3} \tag{73}$$

The right-hand side of this equation is increasing for c between a and b. Thus, as P increases above P_Y the free boundary moves from $c = a$ to eventually reach $c = b$ at the value

$$P = P_{crit} = 2\sigma_Y \log(b/a) \tag{74}$$

To motivate the asymptotics to follow, let us also examine this exact solution in the limit $b - a \ll 1$. Let $b = a + \epsilon d$, $r = a + \epsilon\rho$, $\epsilon \ll 1$. Then, from (58)-(60) we see that

$$\sigma_{rr} \sim -\frac{P(d-\rho)}{d}, \tag{75}$$

$$\sigma_{\theta\theta} \sim \frac{aP}{2\epsilon d}, \tag{76}$$

$$\sigma_{\phi\phi} \sim \frac{aP}{2\epsilon d}, \tag{77}$$

while from (63) we see that P_Y is given by

$$P_Y = \frac{2\sigma_Y \epsilon d}{a}. \tag{78}$$

Thus we see that the pressure required to generate a plastic zone is $O(\epsilon)$, and the stress in the shell is primarily a hoop stress.

Let us now examine the plastic/elastic solution. From (74) we see that to leading order

$$P_{crit} \sim \frac{2\sigma_Y \epsilon d}{a}. \tag{79}$$

Thus $P_{crit} = P_Y$ to leading order in ϵ and we must go to second order to examine the transition from purely elastic to purely plastic. Therefore we set $P = 2\epsilon\sigma_Y d/a + \epsilon^2 \bar{P}$. We also let $c = a + \epsilon\bar{c}$. Then, to leading order throughout the sheet the solution (75)-(77) hold. The quantity of interest is $\bar{c}$, which identifies the point of plastic/elastic transition. Expanding (63) and (74) to two terms gives

$$\bar{P}_Y \sim \frac{2\sigma_Y \epsilon d}{a} - \frac{4\sigma_Y \epsilon^2 d^2}{a^2}, \tag{80}$$

$$P_{crit} \sim \frac{2\sigma_Y \epsilon d}{a} - \frac{\sigma_Y \epsilon^2 d^2}{a^2}. \tag{81}$$

From (73) we find that $\bar{c}$ is given in terms of $\bar{P}$ by

$$\frac{\bar{P}}{\sigma_Y} \sim -\frac{4d^2 - 6d\bar{c} + 3\bar{c}^2}{a^2}. \tag{82}$$

4 Aribtrary cylindrical geometry

Let us now examine a thin cylindrical sheet of uniform thickness ϵd but arbitrary shape. We first note that in the previous sections to leading order the pressure required to initiate a plastic region in the material, P_Y, was the same as that corresponding to a fully plastic material, P_{crit}. Suppose the pressure on the sheet is increased until it becomes plastic and flows. As it flows it will become

thin elastic sheath forms on the outside of the sheet. If the pressure is increased further the sheet will again flow, but it will always stop flowing when the pressure is exactly the critical pressure for that shape of sheet. Thus we might expect the sheet to move quasistatically through critically plastic solutions as the pressure is increased, that is, through solutions in which the whole sheet is plastic and the pressure is exactly equal to the critical pressure P_{crit}.

We are therefore led to ask which shapes are critically plastic for a given pressure, and we will address this quesion in two dimensions in this section. In the following section we will consider three dimensional critically plastic solutions.

We define a curvilinear coordinate system (s, n) by

$$\boldsymbol{x} = \boldsymbol{X}(s) + n\boldsymbol{n}, \tag{83}$$

where $\boldsymbol{X}(s)$ is the inner edge of the sheet, s is arclength, and $\boldsymbol{n}$ is the unit normal, which we take to point from the high-pressure region to the low-pressure region. Then

$$\boldsymbol{x}_s = \boldsymbol{X}_s + n\boldsymbol{n}_s = (1 + \kappa n)\boldsymbol{t}, \tag{84}$$

$$\boldsymbol{x}_n = \boldsymbol{n}, \tag{85}$$

where $\boldsymbol{t}$ is the unit tangent and κ is the curvature of the centreline, positive if the centre of curvature lies in the high-pressure region. Thus our coordinate system is orthogonal, with scaling factors given by

$$h_1 = 1 + \kappa n, \tag{86}$$

$$h_3 = 1 \tag{87}$$

In these curvilinear coordinates the equations of equilibrium, representing force balances in the $\boldsymbol{t}$ and $\boldsymbol{n}$ directions, are

$$\frac{\partial}{\partial s}(\sigma_{11}) + \frac{\partial}{\partial n}(h_1\sigma_{13}) + \frac{\partial h_1}{\partial n}\sigma_{13} = 0, \tag{88}$$

$$\frac{\partial}{\partial s}(\sigma_{13}) + \frac{\partial}{\partial n}(h_1\sigma_{33}) - \frac{\partial h_1}{\partial n}\sigma_{11} = 0, \tag{89}$$

where we have used the index 1 for the tangent and 3 for the normal direction, since in the next section we will include a second tangent direction which will be indexed 2.

We now take advantage of the fact that the sheet is thin, by rescaling $n = \epsilon\rho$ where $\epsilon \ll 1$ and asymptotically expanding as $\epsilon \to 0$ We find that (88), (89) become

$$\frac{\partial}{\partial s}(\sigma_{11}) + \frac{1}{\epsilon}\frac{\partial}{\partial \rho}((1 + \kappa\epsilon\rho)\sigma_{13}) + \kappa\sigma_{13} = 0, \tag{90}$$

with boundary conditions

$$\sigma_{33} = 0, \qquad \sigma_{13} = 0 \text{ on } \rho = d, \tag{92}$$

$$\sigma_{33} = -\epsilon\hat{P}, \qquad \sigma_{13} = 0 \text{ on } \rho = 0. \tag{93}$$

Expanding in powers of ϵ we have

$$\sigma_{11} = \sigma_{11}^{(0)} + \epsilon\sigma_{11}^{(1)} + \cdots, \tag{94}$$

etc. Substituting into (90), (91) gives at leading order

$$\frac{\partial\sigma_{13}^{(0)}}{\partial\rho} = 0, \tag{95}$$

$$\frac{\partial\sigma_{33}^{(0)}}{\partial\rho} = 0. \tag{96}$$

The boundary conditions then imply that

$$\sigma_{13}^{(0)} = 0, \tag{97}$$

$$\sigma_{33}^{(0)} = 0. \tag{98}$$

At next order in (91) we find

$$\frac{\partial\sigma_{33}^{(1)}}{\partial\rho} = \kappa\sigma_{11}^{(0)}. \tag{99}$$

The Tresca condition for the film to be in the plastic state is

$$|\sigma_{11} - \sigma_{33}| = \sigma_Y \tag{100}$$

(for a Von-Mises material we simply replace σ_Y with $2\sigma_Y/\sqrt{3}$). Hence we find that at leading order

$$\sigma_{11}^{(0)} = \pm\sigma_Y. \tag{101}$$

As in the circular case we find that the predominant stress in the sheet is a hoop stress. Since the sheet is in tension we have

$$\sigma_{11}^{(0)} = \sigma_Y. \tag{102}$$

Then

$$\sigma_{33}^{(1)} = \kappa\sigma_Y(\rho - d), \tag{103}$$

where we have used the boundary condition that $\sigma_{33} = 0$ on $\rho = d$. The boundary condition $\sigma_{33} = -\epsilon\hat{P}$ on $\rho = 0$ now gives

$$\hat{P} = d\kappa\sigma_Y. \tag{104}$$

Thus the sheet is behaving exactly as though it were a membrane with tension

5 Arbitrary thin sheets

We will now examine the three-dimensional critically plastic solutions.

Let the inner-surface of the sheet be given by

$$\boldsymbol{x} = \boldsymbol{X}(s_1, s_2). \tag{105}$$

We choose the parametrisation such that lines of constant s_1 and s_2 are the directions of the principal curvatures of the surface. This means that

$$\frac{\partial \boldsymbol{X}}{\partial s_1} \cdot \frac{\partial \boldsymbol{X}}{\partial s_2} = 0 \quad \text{and} \quad \frac{\partial^2 \boldsymbol{X}}{\partial s_1 \partial s_2} = 0, \tag{106}$$

so that the first and second fundamental forms are both diagonal. We define a curvilinear coordinate system (s_1, s_2, n) by

$$\boldsymbol{x} = \boldsymbol{X}(s_1, s_2) + n\boldsymbol{n}(s_1, s_2), \tag{107}$$

where $\boldsymbol{n}$ is the unit normal to the surface, which we again take to point from the high-pressure region to the low-pressure region. This coordinate system is orthogonal, with scaling factors given by

$$h_1 = a_1(1 + \kappa_1 n), \tag{108}$$

$$h_2 = a_2(1 + \kappa_2 n), \tag{109}$$

$$h_3 = 1, \tag{110}$$

where

$$a_1 = \left|\frac{\partial \boldsymbol{X}}{\partial s_1}\right|, \qquad a_2 = \left|\frac{\partial \boldsymbol{X}}{\partial s_2}\right|,$$

and κ_1 and κ_2 are the principal curvatures in the s_1 and s_2 directions respectively (positive if the centre of curvature lies in the high-pressure region).

Force balances in the $\boldsymbol{t}_1$, $\boldsymbol{t}_2$ and $\boldsymbol{n}$ directions give (see, for example, [1, 6])

$$\frac{\partial}{\partial s_1}(h_2\sigma_{11}) + \frac{\partial}{\partial s_2}(h_1\sigma_{12}) + \frac{\partial h_1}{\partial s_2}\sigma_{12} + \frac{\partial}{\partial n}(h_1 h_2 \sigma_{13}) + h_2\frac{\partial h_1}{\partial n}\sigma_{13} - \frac{\partial h_2}{\partial s_1}\sigma_{22} = 0, \tag{111}$$

$$\frac{\partial}{\partial s_1}(h_2\sigma_{12}) + \frac{\partial h_2}{\partial s_1}\sigma_{12} + \frac{\partial}{\partial s_2}(h_1\sigma_{22}) + \frac{\partial}{\partial n}(h_1 h_2 \sigma_{23}) + h_1\frac{\partial h_2}{\partial n}\sigma_{23} - \frac{\partial h_1}{\partial s_2}\sigma_{11} = 0, \tag{112}$$

$$\frac{\partial}{\partial s_1}(h_2\sigma_{13}) + \frac{\partial}{\partial s_2}(h_1\sigma_{23}) + \frac{\partial}{\partial n}(h_1 h_2 \sigma_{33}) - h_2\frac{\partial h_1}{\partial n}\sigma_{11} - h_1\frac{\partial h_2}{\partial n}\sigma_{22} = 0 \tag{113}$$

As before we take advantage of the fact that the sheet is thin by introducing the local scaling $n = \epsilon\rho$. Equations (111)-(113) then become

$$\frac{\partial}{\partial s_1}(a_2\sigma_{11}) + \frac{\partial}{\partial s_2}(a_1\sigma_{12}) + \frac{\partial a_1}{\partial s_2}\sigma_{12} + \frac{a_1a_2}{\epsilon}\frac{\partial}{\partial\rho}((1+\epsilon\kappa_1\rho)(1+\epsilon\kappa_2\rho)\sigma_{13}) + a_1a_2\kappa_1\sigma_{13} - \frac{\partial a_2}{\partial s_1}\sigma_{22} = O(\epsilon), \quad (114)$$

$$\frac{\partial}{\partial s_1}(a_2\sigma_{12}) + \frac{\partial}{\partial s_2}(a_1\sigma_{22}) + \frac{\partial a_2}{\partial s_1}\sigma_{12} + \frac{a_1a_2}{\epsilon}\frac{\partial}{\partial\rho}((1+\epsilon\kappa_1\rho)(1+\epsilon\kappa_2\rho)\sigma_{23}) + a_1a_2\kappa_2\sigma_{23} - \frac{\partial a_1}{\partial s_2}\sigma_{11} = O(\epsilon), \quad (115)$$

$$\frac{\partial}{\partial s_1}(a_2\sigma_{13}) + \frac{\partial}{\partial s_2}(a_1\sigma_{23}) + \frac{a_1a_2}{\epsilon}\frac{\partial}{\partial\rho}((1+\epsilon\kappa_1\rho)(1+\epsilon\kappa_2\rho)\sigma_{33}) - a_1a_2\kappa_1\sigma_{11} - a_1a_2\kappa_2\sigma_{22} = O(\epsilon) \quad (116)$$

Expanding in powers of ϵ as before we find that at leading order

$$\frac{\partial\sigma_{13}^{(0)}}{\partial\rho} = 0, \quad (117)$$

$$\frac{\partial\sigma_{23}^{(0)}}{\partial\rho} = 0, \quad (118)$$

$$\frac{\partial\sigma_{33}^{(0)}}{\partial\rho} = 0 \quad (119)$$

Applying the boundary conditions of zero stress on the outer surface gives

$$\sigma_{13}^{(0)} = 0, \quad (120)$$

$$\sigma_{23}^{(0)} = 0, \quad (121)$$

$$\sigma_{33}^{(0)} = 0 \quad (122)$$

At next order in (116) we find

$$\frac{\partial\sigma_{33}^{(1)}}{\partial\rho} - \kappa_1\sigma_{11}^{(0)} - \kappa_2\sigma_{22}^{(0)} = 0, \quad (123)$$

which we may integrate across the sheet to give

$$P = d(\kappa_1\bar{\sigma}_1 + \kappa_2\bar{\sigma}_2), \quad (124)$$

where a bar represents the average value across the sheet.

At next order in (114)-(115) we find

$$a_1^{(0)}a_2^{(0)}\frac{\partial\sigma_{13}^{(1)}}{\partial\rho} + \frac{\partial a_1^{(0)}}{\partial s_2}\sigma_{12}^{(0)} + \frac{\partial}{\partial s_1}(a_2^{(0)}\sigma_{11}^{(0)})$$

$$\frac{\partial}{\partial}\ {}^{(0)}\ {}^{(0)} \qquad \frac{\partial a_2^{(0)}}{}\ {}^{(0)}$$

$$a_1^{(0)}a_2^{(0)}\frac{\partial\sigma_{23}^{(1)}}{\partial\rho}+\frac{\partial a_2^{(0)}}{\partial s_1}\sigma_{12}^{(0)}+\frac{\partial}{\partial s_1}(a_2^{(0)}\sigma_{12}^{(0)}) + \frac{\partial}{\partial s_2}(a_1^{(0)}\sigma_{22}^{(0)})-\frac{\partial a_1^{(0)}}{\partial s_2}\sigma_{11}^{(0)}=0. \tag{126}$$

Integrating across the sheet we find

$$\frac{\partial a_1^{(0)}}{\partial s_2}\bar{\sigma}_{12}^{(0)}+\frac{\partial}{\partial s_1}(a_2^{(0)}\bar{\sigma}_{11}^{(0)})+\frac{\partial}{\partial s_2}(a_1^{(0)}\bar{\sigma}_{12}^{(0)})-\frac{\partial a_2^{(0)}}{\partial s_1}\bar{\sigma}_{22}^{(0)} = 0, \tag{127}$$

$$\frac{\partial a_2^{(0)}}{\partial s_1}\bar{\sigma}_{12}^{(0)}+\frac{\partial}{\partial s_1}(a_2^{(0)}\bar{\sigma}_{12}^{(0)})+\frac{\partial}{\partial s_2}(a_1^{(0)}\bar{\sigma}_{22}^{(0)})-\frac{\partial a_1^{(0)}}{\partial s_2}\bar{\sigma}_{11}^{(0)} = 0. \tag{128}$$

Equations (127), (128) state that the surface divergence of the surface stress tensor is zero. To apply the plasticity condition we now find it easier to change surface coordinates and work with coordinates associated with the directions of principal stress. Let S_1 and S_2 be such coordinates, and let τ be the stress tensor in this representation. Then (127), (128) become

$$\frac{\partial}{\partial S_1}(\hat{a}_2^{(0)}\bar{\tau}_{11}^{(0)})-\frac{\partial\hat{a}_2^{(0)}}{\partial S_1}\bar{\tau}_{22}^{(0)} = 0, \tag{129}$$

$$\frac{\partial}{\partial S_2}(\hat{a}_1^{(0)}\bar{\tau}_{22}^{(0)})-\frac{\partial\hat{a}_1^{(0)}}{\partial S_2}\bar{\tau}_{11}^{(0)} = 0, \tag{130}$$

where

$$\hat{a}_1=\left|\frac{\partial X}{\partial S_1}\right|, \qquad \hat{a}_2=\left|\frac{\partial X}{\partial S_2}\right|.$$

Let us first consider a Tresca plastic. Since $\tau_{33}^{(0)}=\sigma_{33}^{(0)}=0$ the Tresca condition becomes

$$\max\left(|\tau_{11}^{(0)}-\tau_{22}^{(0)}|,|\tau_{11}^{(0)}|,|\tau_{22}^{(0)}|\right)=\sigma_Y. \tag{131}$$

We now assume that the leading order in-plane stresses are independent of ρ, which will hold if we can think of our expansion in ϵ as equivalent to a Taylor series in the variable n. We may then apply (131) across the sheet. If we assume that the sheet is everywhere under tension the first term cannot be the largest, and the condition reads

$$\max\left(|\bar{\tau}_{11}^{(0)}|,|\bar{\tau}_{22}^{(0)}|\right)=\sigma_Y. \tag{132}$$

Now if $\bar{\tau}_{11}^{(0)}$ is constant the (129) gives $\bar{\tau}_{11}^{(0)}=\bar{\tau}_{22}^{(0)}$, while if $\bar{\tau}_{22}^{(0)}$ is constant the (130) gives $\bar{\tau}_{11}^{(0)}=\bar{\tau}_{22}^{(0)}$. Hence

which implies

$$\bar{\sigma}_{11}^{(0)} = \sigma_Y, \tag{134}$$

$$\bar{\sigma}_{22}^{(0)} = \sigma_Y, \tag{135}$$

$$\bar{\sigma}_{12}^{(0)} = 0. \tag{136}$$

Note that this result does not contradict the two-dimensional result, in which the axial stress was not equal to the hoop stress, because in that case $\hat{a}_1 = \hat{a}_1(S_1)$, $\hat{a}_2 = 1$, so that

$$\frac{\partial \hat{a}_1^{(0)}}{\partial S_2} = 0, \qquad \frac{\partial \hat{a}_2^{(0)}}{\partial S_1} = 0,$$

and we simply have that $\bar{\tau}_{11}^{(0)}$ and $\bar{\tau}_{22}^{(0)}$ are constant. The present analysis only holds in genuinely three-dimensional situations.

Let us now examine a Von-Mises plastic. The Von-Mises condition in three dimensions can be written as

$$(\tau_{11} - \tau_{22})^2 + (\tau_{11} - \tau_{33})^2 + (\tau_{22} - \tau_{33})^2 = 2\sigma_Y^2, \tag{137}$$

where the τ are the principal stresses. To leading order this becomes

$$(\tau_{11}^{(0)} - \tau_{22}^{(0)})^2 + (\tau_{11}^{(0)})^2 + (\tau_{22}^{(0)})^2 = 2\sigma_Y^2, \tag{138}$$

since $\tau_{33}^{(0)} = \sigma_{33}^{(0)} = 0$. If we again assume that the leading order in-sheet stress are independent of ρ then we may write this condition in terms of the stresses integrated over the thickness of the film, giving

$$(\bar{\tau}_{11}^{(0)} - \bar{\tau}_{22}^{(0)})^2 + (\bar{\tau}_{11}^{(0)})^2 + (\bar{\tau}_{22}^{(0)})^2 = 2\sigma_Y^2, \tag{139}$$

In (129), (130) and (139), for a given sheet shape, we now have three equations for the two unknowns $\bar{\tau}_{11}^{(0)}$ and $\bar{\tau}_{22}^{(0)}$, for which the only solution is again given by (133). Thus we again arrive at (134)-(136)

Finally, using (134)-(136), equation (124) becomes

$$P = d\kappa\sigma_Y, \tag{140}$$

where $\kappa = \kappa_1 + \kappa_2$ is the mean curvature of the sheet.

6 Evolution of the sheet in two-dimensions

Let us now examine the quasistatic evolution of the shape of the sheet as P is increased, under the condition for equilibrium that

$$P = d\kappa\sigma_Y. \tag{141}$$

We consider the problem of an initially flat sheet (i e for $P = 0$) being sucked into a rectangular mould, as shown in Figure 5 We assume that a plastic hinge is formed at A and B in Figure 5, so that the sheet is pinned there but the angle

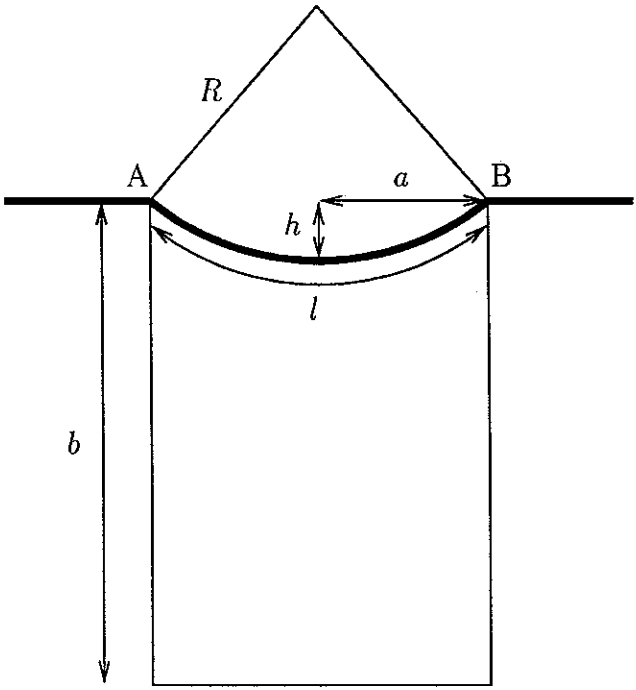

Figure 5: The geometry of the sheet

6.1 Constant d

If d is taken to be constant, equal to d_0 say, then the shapes of the sheet are simply arcs of circles. If the radius of curvature is R, the semiwidth of the opening is a, and the depth of deflection is h, then (see Figure 5)

$$h = R - \sqrt{R^2 - a^2}, \tag{142}$$

$$R = \frac{d_0 \sigma_Y}{P}, \tag{143}$$

and therefore

$$h = \frac{d_0 \sigma_Y}{P} - \sqrt{\frac{d_0^2 \sigma_Y^2}{P^2} - a^2}. \tag{144}$$

For small P, the initial deflection is given approximately by

$$h \sim \frac{a^2}{2} \frac{P}{d_0 \sigma_Y} + \frac{a^4}{8} \left(\frac{P}{d_0 \sigma_Y} \right)^3, \tag{145}$$

which is quadratic in the semiwidth a to leading order as expected.

To plot the results it makes sense to write them in dimensionless form. Using

$$P_* \qquad P \qquad h$$

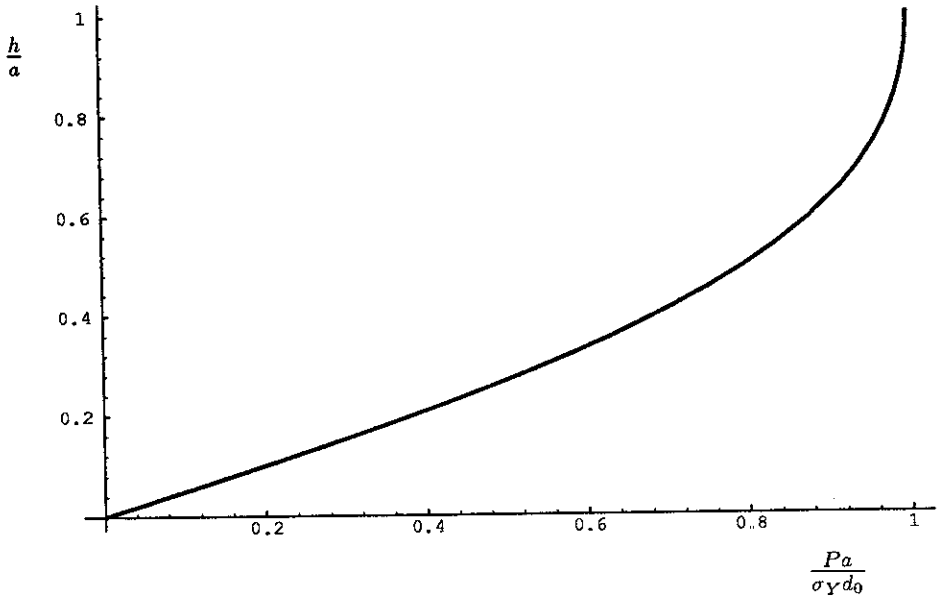

Figure 6: Dimensionless displacement as a function of dimensionless pressure

as dimensionless pressure, radius of curvature and depth respectively we have

$$h' = \frac{1}{P'} - \sqrt{\frac{1}{(P')^2} - 1}, \tag{146}$$

which is shown in Figure 6.

A second quantity of interest is the relationship between the displacement h and the semiwidth a for various pressures. We write

$$\frac{Ph}{d_0\sigma_Y} = 1 - \sqrt{1 - \frac{1}{(R')^2}}, \tag{147}$$

$$\frac{Pa}{d_0\sigma_Y} = \frac{1}{R'} \tag{148}$$

Thus we see that the nondimensional quantities of interest are

$$\frac{Ph}{d_0\sigma_Y} \quad \text{and} \quad \frac{Pa}{d_0\sigma_Y}.$$

The relationship (147), (148) is plotted in Figure 7.

It is of interest to note the scaling law implied by (147), (148), which indicates that the graphs of h versus a for different pressures can all be collapsed onto

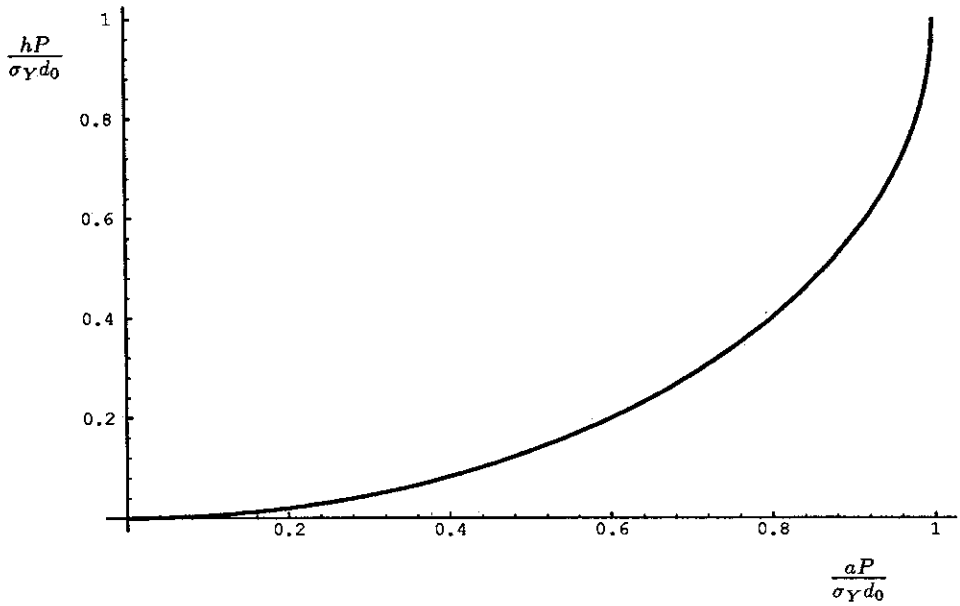

Figure 7: Dimensionless displacement as a function of dimensionless semiwidth

6.2 Uniform d

Of course, in reality the sheet will thin as it stretches Let us now suppose that the thickness of the sheet is still uniform, but that the sheet thins by mass conservation. Then, for a given deflection, the thickness is determined by the equation

$$ld = 2ad_0, \tag{149}$$

where l is the length of the sheet. Since d is uniform the shapes of the sheet are still arcs of circles. With the same notation as above we have

$$l = 2R\sin^{-1}(a/R), \tag{150}$$

$$d = \frac{d_0 a}{R\sin^{-1}(a/R)}, \tag{151}$$

$$h = R - \sqrt{R^2 - a^2}, \tag{152}$$

$$P = \frac{d_0 a \sigma_Y}{R^2 \sin^{-1}(a/R)}. \tag{153}$$

Equations (152) and (153) give the relationship between P and h parametrically; we cannot easily write R as a function of P in this case (although we may

the initial deflection for small P (large R) we find

$$h \sim \frac{a^2}{2R} + \frac{a^4}{8R^3}, \tag{154}$$

$$P \sim \frac{d_0\sigma_Y}{a}\left(\frac{a}{R} - \frac{a^3}{6R^3}\right). \tag{155}$$

Hence

$$h \sim \frac{a^2}{2}\frac{P}{d_0\sigma_Y} + \frac{5a^4}{24}\left(\frac{P}{d_0\sigma_Y}\right)^3. \tag{156}$$

Comparing (156) to (145) we see that the thinning does not alter the first term in the expansion, but does give a greater deflection in the second term, as we would expect.

To plot the results we use the same nondimensionalisations as above. We have then

$$P' = \frac{1}{(R')^2 \sin^{-1}(1/R')}, \tag{157}$$

$$h' = R' - \sqrt{(R')^2 - 1} \tag{158}$$

The graph of nondimensional displacement versus nondimensional pressure is shown in Figure 8.

We see that the graph turns around on itself, that is, for values of P greater that a critical value P_c there is no solution. This critical situation arises because the increase in pressure the sheet can withstand due to its increase in curvature is less than the decrease in pressure due to the fact that it thins. As P increases through P_c we would expect there to be a large change in the shape of the sheet, which would flow until it touched the base of the mould. We would then expect the new shape to be of the form considered in the next section

We can calculate the value of P_c from (157), (158). We find the critical point corresponds to

$$R'_c \approx 1.08813, \qquad P'_c \approx 0.724611, \qquad h'_c \approx 0.65915,$$

which, in dimensional variables, is

$$R_c = 1\ 08813\, a, \qquad P_c = \frac{0.724611\, \sigma_Y d_0}{a}, \qquad h_c = 0\ 65915\, a \tag{159}$$

This is because the increased pressure the sheet can withstand due to the increase in curvature is less than the decrease in pressure it can withstand due to it thinning beyond this point.

It is again of interest to examine the displacement as a function of the semiwidth. We find

$$\frac{hP}{d_0\sigma_Y} = \frac{R' - \sqrt{(R')^2 - 1}}{(R')^2 \sin^{-1}(1/R')}, \tag{160}$$

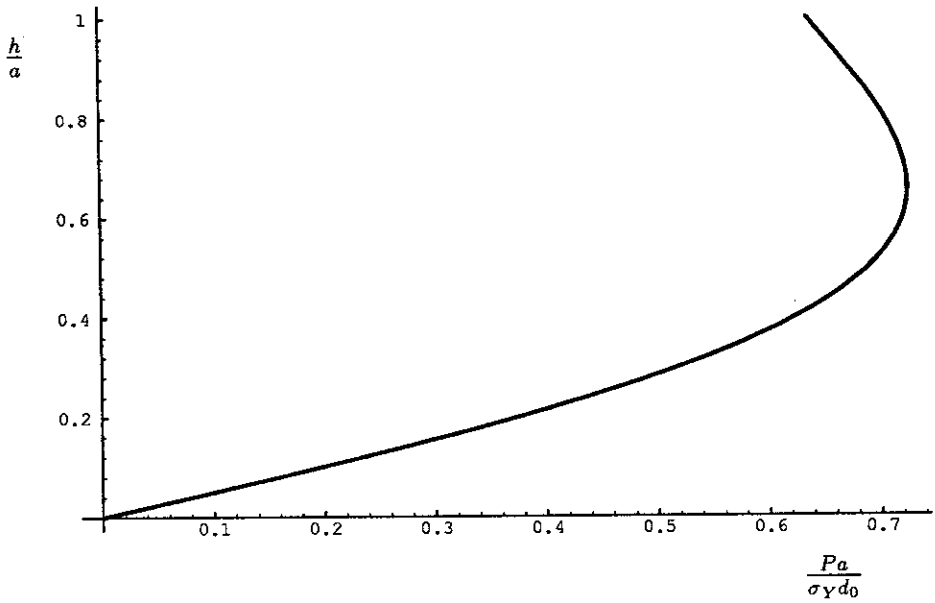

Figure 8: Dimensionless displacement as a function of dimensionless pressure

Thus the same scaling law holds, so that the curves for different pressures can be collapsed to a single curve by plotting the correct nondimensional parameters. The curves (160), (161) are shown in Figure 9.

6.3 Corners

The preceding analysis holds until the radius of curvature of the sheet is equal to the semiwidth. At this stage there is nothing to prevent the sheet expanding until it meets the bottom of the mould. At this value of P, with no thinning of the film, the semicircular part of the sheet may be at any height in the mould. With thinning, the only stable position will be with the semicircle touching the bottom of the mould. Let us now increase the pressure further and see how far the sheet makes it into the corners of the mould.

Constant d. The sheet will meet the sides of the mould tangentially (see Figure 10) Hence, with no thinning the final radius of curvature in the corners, R, is simply given by

$$R = \frac{d_0 \sigma_Y}{P}. \tag{162}$$

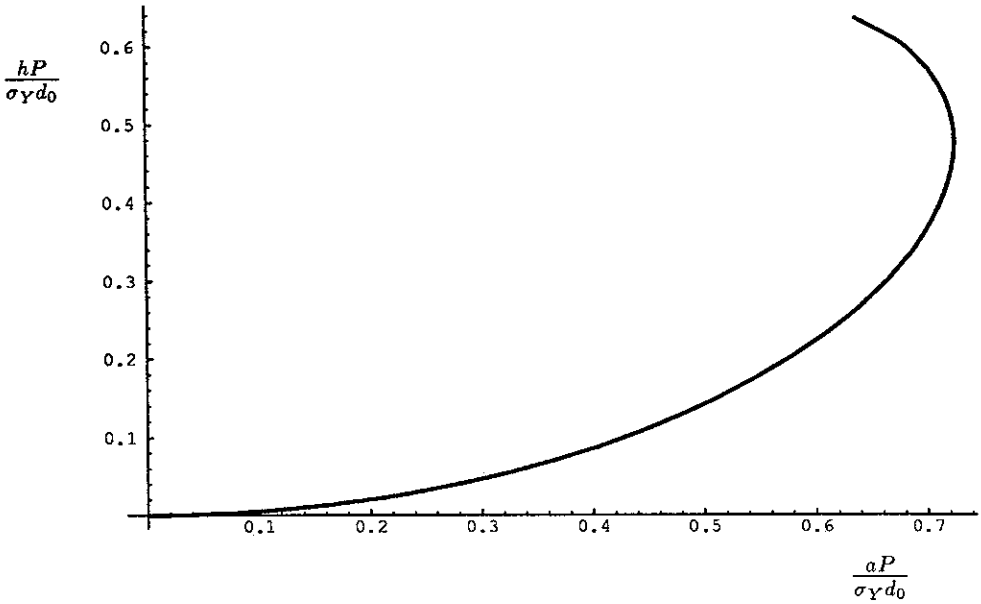

Figure 9: Dimensionless displacement as a function of dimensionless semiwidth

Uniform d. If we assume uniform thinning of the sheet, then the length is given by

$$l = 2(b - R) + 2(a - R) + \pi R, \tag{163}$$

where b is the depth of the mould. Hence the thickness is given by

$$d = \frac{2ad_0}{2b + 2a + (\pi - 4)R} \tag{164}$$

Therefore we find that

$$P = \frac{2ad_0\sigma_Y}{R(2b + 2a + (\pi - 4)R)} \tag{165}$$

7 Evolution of the sheet in three dimensions

If the opening of the mould is a circle, then for uniform d the shapes taken by the sheet during the initial part of its quasistatic evolution will be sections of spheres, and we can perform an analysis exactly similar to that of Section 6

7.1 Constant d

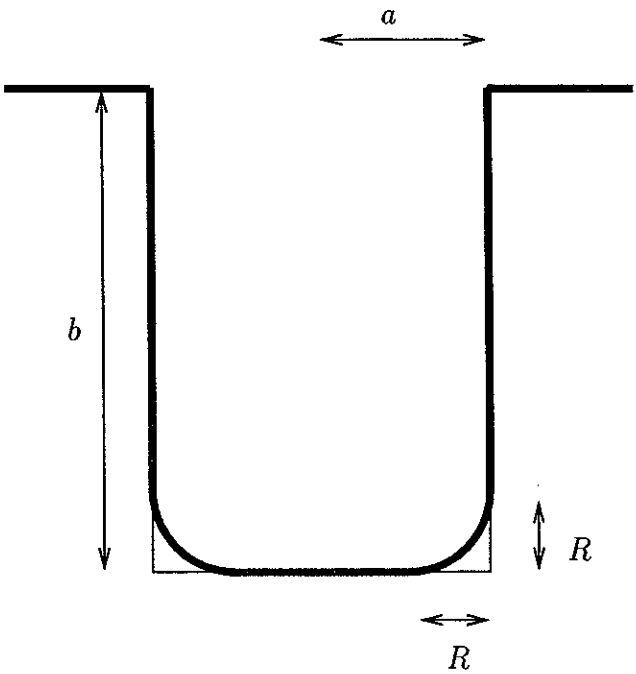

Figure 10· The geometry of the sheet

deflection is h, then

$$h = R - \sqrt{R^2 - a^2}, \tag{166}$$

$$R = \frac{2d_0\sigma_Y}{P}, \tag{167}$$

and therefore

$$h = \frac{2d_0\sigma_Y}{P} - \sqrt{\frac{4d_0^2\sigma_Y^2}{P^2} - a^2}. \tag{168}$$

For small P, the initial deflection is given approximately by

$$h \sim \frac{a^2}{4}\frac{P}{d_0\sigma_Y} + \frac{a^4}{64}\left(\frac{P}{d_0\sigma_Y}\right)^3. \tag{169}$$

We see that the effect of the third dimension is the factor of 2 in equation (167), with the result that twice the pressure is needed to obtain the same deflection as the two-dimensional case.

Using

$$P' = \frac{Pa}{\sigma_Y d_0}, \qquad R' = \frac{R}{a}, \qquad h' = \frac{h}{a},$$

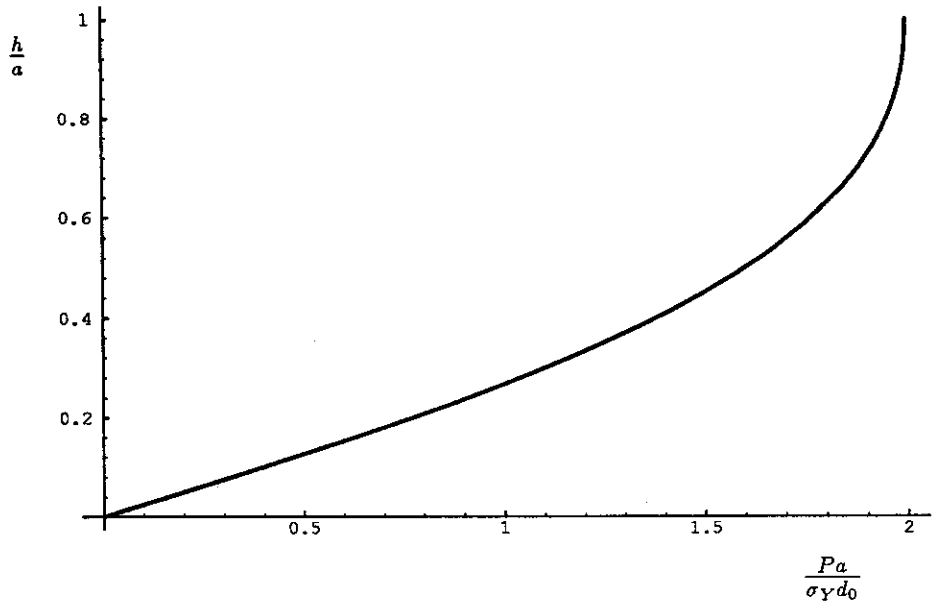

Figure 11: Dimensionless displacement as a function of dimensionless pressure

we have

$$h' = \frac{2}{P'} - \sqrt{\frac{4}{(P')^2} - 1}, \tag{170}$$

which is shown in Figure 11.

Let us now turn to the relationship between the displacement h and the semiwidth a for various pressures. As before we write

$$\frac{Ph}{d_0\sigma_Y} = 2\left(1 - \sqrt{1 - \frac{1}{(R')^2}}\right), \tag{171}$$

$$\frac{Pa}{d_0\sigma_Y} = \frac{2}{R'}. \tag{172}$$

The relationship (147), (148) is plotted in Figure 12

Note that the same scaling law applies in three dimensions as in two dimensions.

7.2 Uniform d

Let us now suppose that the thickness of the sheet is still uniform, but that the

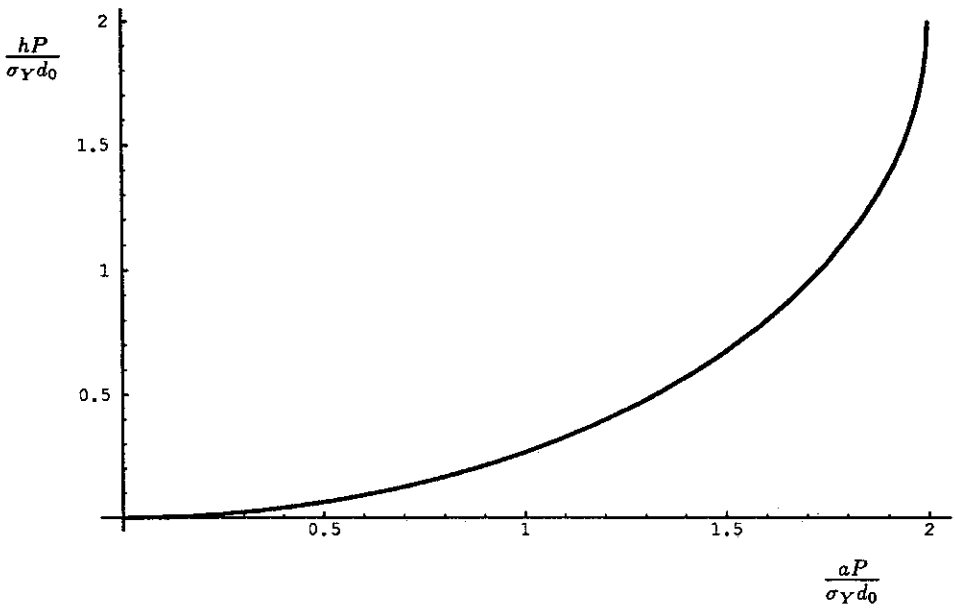

Figure 12: Dimensionless displacement as a function of dimensionless semiwidth

determined by the equation

$$Ad = \pi a^2 d_0, \tag{173}$$

where A is the area of the sheet. Since d is uniform the shapes of the sheet are still sections of spheres. With the same notation as above we have

$$A = 2\pi R\left(R - \sqrt{R^2 - a^2}\right), \tag{174}$$

$$d = \frac{d_0 a^2}{2R\left(R - \sqrt{R^2 - a^2}\right)}, \tag{175}$$

$$h = R - \sqrt{R^2 - a^2}, \tag{176}$$

$$P = \frac{d_0 a^2 \sigma_Y}{R^2\left(R - \sqrt{R^2 - a^2}\right)}. \tag{177}$$

Equations (176) and (177) give the relationship between P and h parametrically; we cannot easily write R as a function of P, although we could eliminate R to give h implicitly as a function of P is so desired. If we examine the initial deflection for small P (large R) we find

$$\frac{a^2}{} \qquad \frac{a^4}{}$$

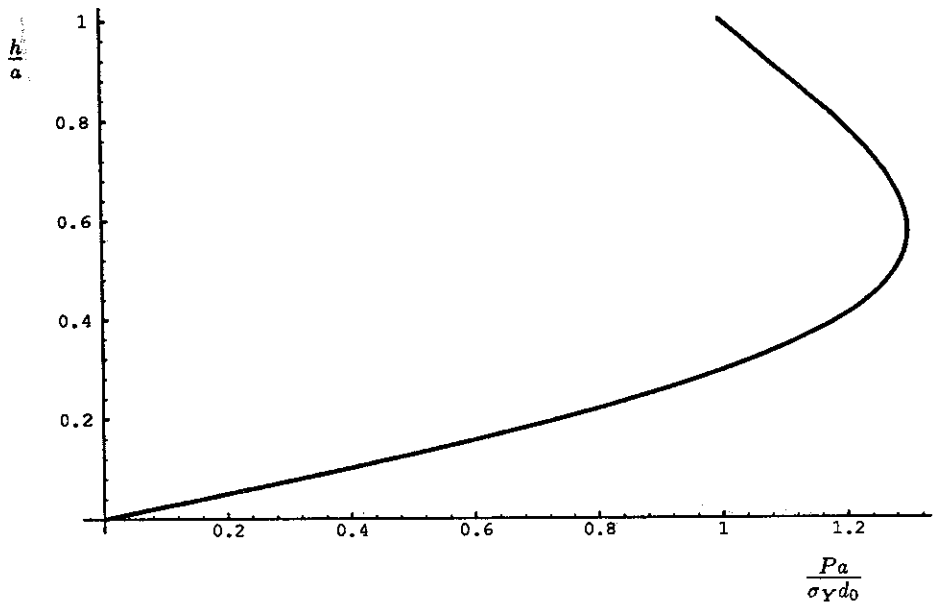

Figure 13: Dimensionless displacement as a function of dimensionless pressure

$$P \sim \frac{d_0\sigma_Y}{a}\left(\frac{2a}{R} - \frac{a^3}{2R^3}\right). \tag{179}$$

Hence

$$h \sim \frac{a^2}{4}\frac{P}{d_0\sigma_Y} + \frac{a^4}{32}\left(\frac{P}{d_0\sigma_Y}\right)^3. \tag{180}$$

Comparing (180) to (169) we see that the thinning does not alter the first term in the expansion, but does give a greater deflection in the second term, as we would expect.

To plot the results we use the same nondimensionalisations as above. We have then

$$P' = \frac{1}{(R')^2\left(R' - \sqrt{(R')^2 - 1}\right)}, \tag{181}$$

$$h' = R' - \sqrt{(R')^2 - 1}. \tag{182}$$

The graph of nondimensional displacement versus nondimensional pressure is shown in Figure 13.

We see as in the two-dimensional case that the graph turns around on itself;

the sheet, which would flow until it touched the base of the mould. We would then expect the new shape to be of the form considered in the next section.

We can calculate the value of P_c from (181), (182). We find the critical point corresponds to

$$R'_c = 2/\sqrt{3}, \qquad P'_c = 3\sqrt{3}/4, \qquad h'_c = 1/\sqrt{3},$$

which, in dimensional variables, is

$$R_c = \frac{2a}{\sqrt{3}}, \qquad P_c = \frac{3\sqrt{3}\,\sigma_Y d_0}{4a}, \qquad h_c = \frac{a}{\sqrt{3}}. \tag{183}$$

It is again of interest to examine the displacement as a function of the semiwidth. We find

$$\frac{hP}{d_0\sigma_Y} = \frac{1}{(R')^2}, \tag{184}$$

$$\frac{aP}{d_0\sigma_Y} = \frac{1}{(R')^2\left(R' - \sqrt{(R')^2 - 1}\right)}. \tag{185}$$

Thus the same scaling law holds, so that the curves for different pressures can be collapsed to a single curve by plotting the correct nondimensional parameters. The curves (184), (185) are shown in Figure 14.

7.3 Corners

As the sheet is pushed into the corners its curved section will correspond to a body of revolution with constant mean curvature. If we let the position of the sheet be described by

$$\boldsymbol{x} = ((a + f(y))\cos\theta, (a + f(y))\sin\theta, y)\,, \tag{186}$$

then we find that the first and second fundamental forms defined by

$$E = \boldsymbol{x}_\theta \cdot \boldsymbol{x}_\theta, \qquad F = \boldsymbol{x}_\theta \cdot \boldsymbol{x}_y, \qquad G = \boldsymbol{x}_y \cdot \boldsymbol{x}_y,$$

$$\boldsymbol{n} = \frac{1}{|\boldsymbol{x}_\theta \wedge \boldsymbol{x}_y|}\boldsymbol{x}_\theta \wedge \boldsymbol{x}_y,$$

$$L = \boldsymbol{x}_{\theta\theta} \cdot \boldsymbol{n}, \qquad M = \boldsymbol{x}_{\theta y} \cdot \boldsymbol{n}, \qquad N = \boldsymbol{x}_{yy} \cdot \boldsymbol{n},$$

are given by

$$E = (a + f)^2, \qquad F = 0, \qquad G = 1 + (f')^2, \tag{187}$$

$$L = -\frac{(a + f)}{(1 + (f')^2)^{1/2}}, \qquad M = 0, \qquad N = \frac{f''}{(1 + (f')^2)^{1/2}}, \tag{188}$$

where a prime represents d/dy. The mean curvature is given by

$$\frac{f''}{} \qquad \frac{1}{} \qquad (189)$$

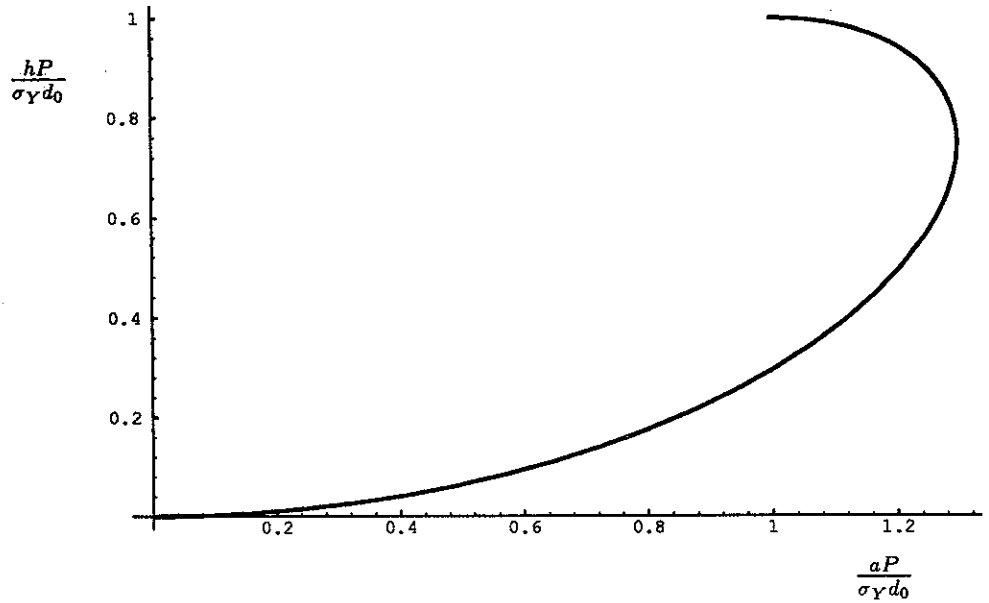

Figure 14: Dimensionless displacement as a function of dimensionless semiwidth

The boundary conditions on this equation are

$$f(0) = -R_1, \qquad f'(0) = \infty, \qquad f(R_2) = 0, \qquad f'(R_2) = 0, \tag{190}$$

which state that the sheet meets the mould tangentially at a height R_2 on the outer wall and at a radius R_1 on the bottom wall (see Figure 15).

We nondimensionalise by setting $f = aF$, $y = aY$, to give

$$\frac{aP}{d\sigma_Y} = -\frac{F''}{(1+(F')^2)^{3/2}} + \frac{1}{(1+F)(1+(F')^2)^{1/2}}, \tag{191}$$

with boundary conditions

$$F(0) = -R_1/a, \qquad F'(0) = \infty, \qquad F(R_2/a) = 0, \qquad F'(R_2/a) = 0, \tag{192}$$

where a prime now represents d/dY, and we have used equation (140).

When we ignore the fact that the sheet thins d is equal to the constant value d_0. In this case we have solved (191) numerically for various values of $aP/d\sigma_Y$. A typical sheet profile is shown in Figure 16. Figure 17 shows R_1/a and R_2/a as a function of $aP/d\sigma_Y$. The value $aP/d\sigma_Y = 2$, gives $R_1 = R_2 = a$, and corresponds to the sheet being a hemispherical shell which just touches the

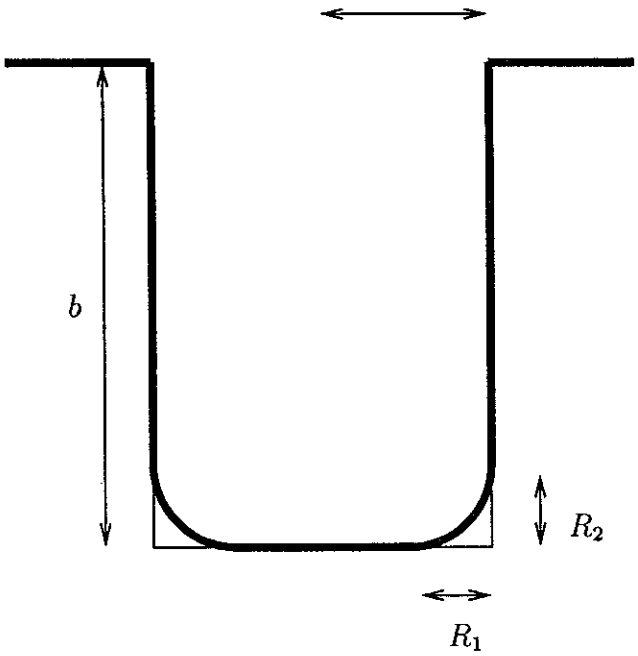

Figure 15: The geometry of the sheet

When we include the thinning of the sheet, but still take d to be uniform, d in (191) is an unknown which is coupled to the shape f through the equation

$$d \times \text{Area of sheet} = d_0 \pi a^2,$$

which may be written

$$d\left[\left(1-\frac{R_1}{a}\right)^2 + 2\left(\frac{b}{a}-\frac{R_2}{a}\right) + 2\int_0^{R_2/a} (1+F)\left(1+(F')^2\right)^{1/2}\, dY\right] = d_0. \tag{193}$$

However, these equations are not really coupled. The left-hand side of (191) is still constant. For a given value of this constant we can solve (191). We can then use (193) to determine the value of d, and this then in turn gives us the corresponding value of P.

8 Non-uniform thinning

8.1 Two dimensions

Let the position of the sheet be given parametrically by

$$x = (x(s), y(s)) \tag{194}$$

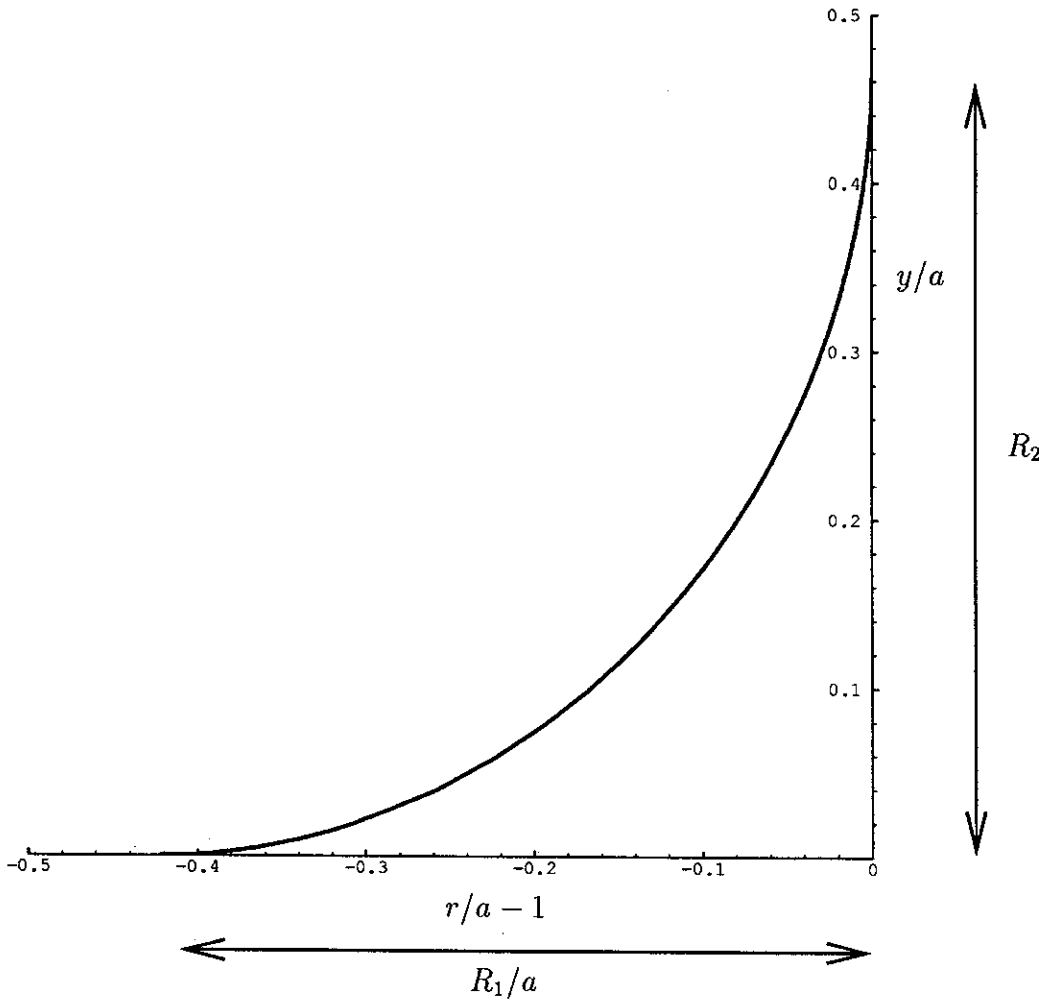

Figure 16: The shape of the sheet for $aP/d_0\sigma_Y = 3$.

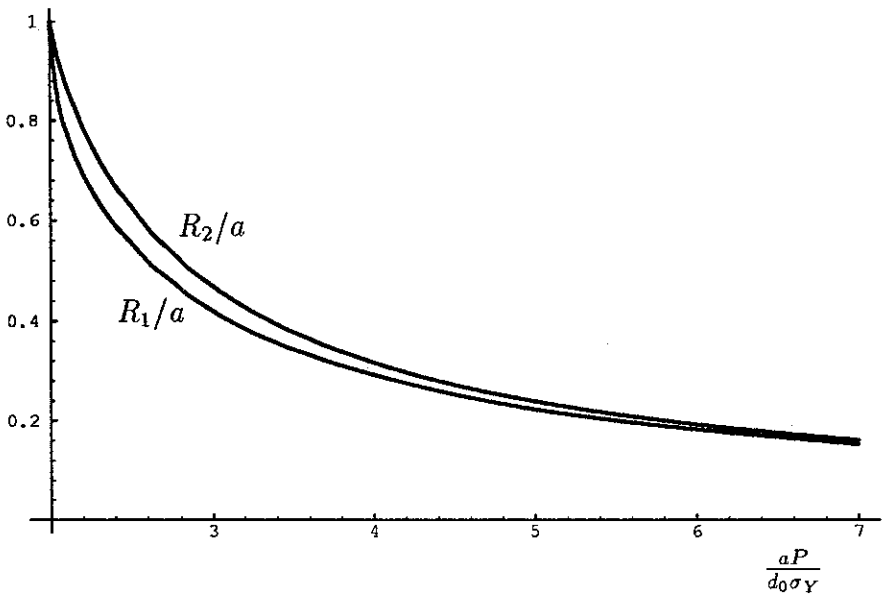

Figure 17. R_1/a and R_2/a as a function of $aP/d_0\sigma_Y$

Then we have our equation of equilibrium

$$P = \kappa(s)d(s)\sigma_Y. \tag{195}$$

As the curve lengthens the sheet will thin. Conservation of area gives

$$d(s)\left(x_s^2 + y_s^2\right)^{1/2} = d_0. \tag{196}$$

Finally, we need an equation to say how the curve stretches. We assume that the material flows normal to the curve. This gives the final equation

$$(x_s, y_s) \cdot (x_t, y_t) = 0. \tag{197}$$

Using the expression

$$\kappa = \frac{x_s y_{ss} - y_s x_{ss}}{(x_s^2 + y_s^2)^{3/2}}, \tag{198}$$

we then have

$$\frac{d_0(x_s y_{ss} - y_s x_{ss})}{(x_s^2 + y_s^2)^2} = P, \tag{199}$$

In (199) P is a given function of time, but in fact we may take $P = t$ without loss of generality. It is better to think of P as a parameter and to write equation (200) as

$$x_s x_P + y_s y_P = 0. \tag{201}$$

8.2 Three dimensions

Let the position of the sheet be given parametrically by

$$\boldsymbol{x} = (x(s_1, s_2), y(s_1, s_2), z(s_1, s_2)). \tag{202}$$

Then we have our equation of equilibrium

$$P = \kappa(s_1, s_2) d(s_1, s_2) \sigma_Y. \tag{203}$$

As the sheet stretches it will thin. Conservation of volume gives

$$d(s_1, s_2) \left(EG - F^2\right)^{1/2} = d_0, \tag{204}$$

where E, F and G are the first fundamental form, defined after (186), and $\left(EG - F^2\right)^{1/2}$ is the area element. Finally, we need an equation to say how the curve stretches. As in two dimensions, we assume that the material flows normal to the curve This gives the final equations

$$(x_{s_1}, y_{s_1}, z_{s_1}) \cdot (x_t, y_t, z_t) = 0, \tag{205}$$

$$(x_{s_2}, y_{s_2}, z_{s_2}) \ (x_t, y_t, z_t) = 0 \tag{206}$$

9 Viscous fluid

We note that an alternative way of modelling the material in the process under consideration is as a viscous fluid The problem then corresponds to the problem of glass blowing, which has been studied recently in [3]

The equations for the leading order stress in the sheet follow exactly as before, so that (124), (129) and (130) still hold. Now, however, instead of closing these equations with a plasticity condition, they are closed by relating the stress to the fluid velocity, giving

$$\bar{\sigma}_{11} = \frac{2\mu d}{a_1 a_2} \left[2 \left(a_2 \frac{\partial a_1}{\partial t} + \tilde{u}_2 \frac{\partial a_1}{\partial s_2} + a_2 \frac{\partial \tilde{u}_1}{\partial s_1} \right) + \left(a_1 \frac{\partial a_2}{\partial t} + \tilde{u}_1 \frac{\partial a_2}{\partial s_1} + a_1 \frac{\partial \tilde{u}_2}{\partial x_2} \right) \right], \tag{207}$$

$$\bar{\sigma}_{22} = \frac{2\mu d}{a_1 a_2} \left[\left(a_2 \frac{\partial a_1}{\partial t} + \tilde{u}_2 \frac{\partial a_1}{\partial s_2} + a_2 \frac{\partial \tilde{u}_1}{\partial s_1} \right) + 2 \left(a_1 \frac{\partial a_2}{\partial t} + \tilde{u}_1 \frac{\partial a_2}{\partial s_1} + a_1 \frac{\partial \tilde{u}_2}{\partial x_2} \right) \right], \tag{208}$$

$$+ \left[\frac{\partial \tilde{u}}{\partial} \right. \quad \left. \frac{\partial \tilde{u}}{\partial} \right]$$

where $\tilde{u}_1$ and $\tilde{u}_2$ is the velocity of the fluid relative to the velocity of the sheet. To these equations must be added the equation of conservation of mass

$$\frac{\partial}{\partial t}(a_1 a_2 d) + \frac{\partial}{\partial s_1}(\tilde{u}_1 a_2 d) + \frac{\partial}{\partial s_2}(\tilde{u}_2 a_1 d) = 0 \tag{210}$$

The system is closed by adding the geometrical relationships

$$a_1 \frac{\partial \kappa_1}{\partial s_2} = (\kappa_2 - \kappa_1)\frac{\partial a_1}{\partial s_2}, \tag{211}$$

$$a_2 \frac{\partial \kappa_2}{\partial s_1} = (\kappa_1 - \kappa_2)\frac{\partial a_2}{\partial s_1}, \tag{212}$$

$$\frac{\partial}{\partial s_1}\left(\frac{1}{a_1}\frac{\partial a_2}{\partial x_1}\right) + \frac{\partial}{\partial s_2}\left(\frac{1}{a_2}\frac{\partial a_1}{\partial x_2}\right) + a_1 a_2 \kappa_1 \kappa_2 = 0 \tag{213}$$

These equations are formidable, although progress can be made in some cases by taking advantage of symmetry, for example in the case of circularly cylindrical shells and spherical shells; the reader is referred to [3].

10 Conclusion

Working on the hypothesis that the sheet will be in a critically plastic state whenever it stops flowing, we have systematically derived a model for the final shape of a sheet subjected to a given pressure drop by performing an asymptotic expansion as the thickness of the sheet tends to zero. In Section 4 we considered two-dimensional situations, while in Section 5 we considered fully three-dimensional situations In Sections 6 and 7 we examined the predictions of this model for the dependence of the final displacement of the sheet on both applied pressure and the dimensions of the opening of the mould, under the assumption that the thickness of the sheet remained uniform. The analysis highlighted certain nondimensional groups as being the important parameters; it will be interesting to see if the experimental data can be collapsed onto a single curve by rescaling as this analysis suggests. We also considered the question of how far into the corners of the mould the sheet will be pushed for a given pressure drop

In Section 8 we derived a model which would allow the thickness of the sheet to vary spatially as well as temporally as the material was stretched

Finally, in Section 9, we briefly considered an alternative formulation in which the sheet is modelled as a viscous fluid rather than a plastic.

References

[1] Aris, R , *Vectors, tensors, and the basic equations of fluid mechanics*, Prentice-Hall (1962). (Reprinted 1989 Dover)

[2] Calladine, C R , *Plasticity for engineers*, Ellis Horwood Series in Engineering

[3] van de Fliert, B.W., Howell, P.D. & Ockendon, J.R., "Pressure-driven flow of a thin viscous sheet", *J. Fluid Mech.*, **292**, 359–376 (1995).

[4] Hill, R., *The mathematical theory of plasticity*, Oxford University Press (1950).

[5] Lubliner, J., *Plasticity Theory*, Macmillan Publishing Company, New York (1990).

[6] Rosenhead, L., *Laminar boundary layers*, Clarendon Press, Oxford (1963).

[7] Sherby, O.D., Nieh, T.G. & Wadsworth, J., "Overview on Superplasticity Research on Small-Grained Materials," In the proceedings of the 1994 International Conference on Superplasticity in Advanced Materials, (ICSAM-94), May 24-26, Moscow (1994)